Cell

MafB Restricts M-CSF-Dependent Myeloid Commitment Divisions of Hematopoietic Stem Cells

Sandrine Sarrazin,[1,2,3] Noushine Mossadegh-Keller,[1,2,3,9] Taro Fukao,[1,2,3,5,9] Athar Aziz,[1,2,3,6] Frederic Mourcin,[1,2,3,7] Laurent Vanhille,[1,2,3] Louise Kelly Modis,[1,2,3,8] Philippe Kastner,[4] Susan Chan,[4] Estelle Duprez,[1,2,3] Claas Otto,[1,2,3] and Michael H. Sieweke[1,2,3,*]

[1]Centre d'Immunologie de Marseille-Luminy (CIML), Université Aix-Marseille, Campus de Luminy, Case 906, 13288 Marseille Cedex 09, France

[2]Institut National de la Santé et de la Recherche Médicale (INSERM), U631, Marseille, France

[3]Centre National de la Recherche Scientifique (CNRS), UMR6102, Marseille, France

[4]Institut de Génétique et de Biologie Moléculaire et Cellulaire, Université de Strasbourg, Strasbourg F-67000, France

[5]Present address: Max-Planck Institute of Immunobiology, Stübeweg 51, D-79108 Freiburg, Germany

[6]Present address: Department of Haematology, Cambridge Institute for Medical Research, University of Cambridge, Hills Road, Cambridge CB2 0XY, UK

[7]Present address: INSERM U917, Faculté de Médecine, Université de Rennes, Rennes F-35043, France

[8]Present address: Boehringer Ingelheim Pharmaceuticals, Inc., 900 Ridgebury Road, Ridgefield, CT 06877, USA

[9]These authors contributed equally to this work

*Correspondence: sieweke@ciml.univ-mrs.fr

DOI 10.1016/j.cell.2009.04.057

SUMMARY

While hematopoietic stem cell (HSC) self-renewal is well studied, it remains unknown whether distinct control mechanisms enable HSC divisions that generate progeny cells with specific lineage bias. Here, we report that the monocytic transcription factor MafB specifically restricts the ability of M-CSF to instruct myeloid commitment divisions in HSCs. MafB deficiency specifically enhanced sensitivity to M-CSF and caused activation of the myeloid master-regulator PU.1 in HSCs in vivo. Single-cell analysis revealed that reduced MafB levels enabled M-CSF to instruct divisions producing asymmetric daughter pairs with one PU.1^{+} cell. As a consequence, *MafB*$^{-/-}$ HSCs showed a PU.1 and M-CSF receptor-dependent competitive repopulation advantage specifically in the myelomonocytic, but not T lymphoid or erythroid, compartment. Lineage-biased repopulation advantage was progressive, maintained long term, and serially transplantable. Together, this indicates that an integrated transcription factor/cytokine circuit can control the rate of specific HSC commitment divisions without compromising other lineages or self-renewal.

INTRODUCTION

The different short-lived cell types of mammalian blood are continuously regenerated from a small population of hematopoietic stem cells (HSCs) in the bone marrow (Bryder et al., 2006). Although a significant proportion of HSCs with long-term reconstitution potential is predominantly quiescent or divides infrequently (Wilson et al., 2008), HSCs need to enter the cycle to continuously regenerate mature blood cells in a correctly balanced ratio or to replenish the stem cell pool under stress conditions. Cell division of HSCs may thus result in self-renewal divisions or the production of more differentiated progeny (Orford and Scadden, 2008). Although such downstream progenitors still retain a high degree of multipotency, recent advances in their characterization also suggest that early diversification into cells with distinct lineage bias can occur at the most primitive stem and precursor cell level (Dykstra et al., 2007; Iwasaki and Akashi, 2007; Luc et al., 2008). However, the mechanisms controlling such specific lineage engagement divisions remain elusive.

Several cellular regulators have been identified that can either promote or restrict HSC cycling, but their mutation in genetic models exclusively affected self-renewal (Orford and Scadden, 2008; Zon, 2008). By contrast, regulators that selectively control lineage-specific commitment divisions of HSCs have not been identified. In this context, the importance of both transcription factor and cytokine signaling for lineage engagement has been invoked (Metcalf, 2007, 2008; Orkin and Zon, 2008; Sieweke and Graf, 1998; Zhang and Lodish, 2008), but no clear mechanism has emerged as to how these two critical control elements might be integrated. Transcription factors with effects on stem cell cycling so far were exclusively found to affect self-renewal divisions (Orford and Scadden, 2008; Zon, 2008). As for cytokine receptors, several of them are expressed on primitive hematopoietic stem and precursor cells (Akashi et al., 2003; Hu et al., 1997; Miyamoto et al., 2002), but it has been a long-standing debate whether cytokine signaling has instructive or permissive

effects on lineage commitment (Enver et al., 1998; Metcalf, 1998). On the one hand, observations that differentiation can occur in the absence of lineage-specific cytokine signaling and that ectopic receptor expression can induce proliferation without commitment to the cytokine affiliated pathway (Enver et al., 1998; Lagasse and Weissman, 1997; McArthur et al., 1994; Metcalf, 2008) have been interpreted as a permissive role of cytokine signaling in lineage engagement. On the other hand, examples have been reported where ectopic cytokine signals resulted in lineage conversion and thus supported an instructive model (Kondo et al., 2000; Pawlak et al., 2000).

MafB is a bZip type transcription factor that is highly expressed in mature monocytes and macrophages (Eichmann et al., 1997; Kelly et al., 2000; Sieweke et al., 1996). Overexpression of MafB limits myeloid progenitor proliferation (Tillmanns et al., 2007) and accelerates macrophage differentiation (Gemelli et al., 2006; Kelly et al., 2000) at the expense of other cell fate options (Bakri et al., 2005; Sieweke et al., 1996). Furthermore, MafB-deficient macrophages show increased responsiveness to M-CSF-induced morphological changes (Aziz et al., 2006). M-CSF has been mainly characterized for its lineage-specific effects on monocytes and macrophages (Pixley and Stanley, 2004), but earlier work also suggested that M-CSF can act on primitive stem and precursor cell populations (Kriegler et al., 1994), which upon more detailed characterization were also found to express its receptor (Akashi et al., 2003; Miyamoto et al., 2002).

Here, we report that MafB deficiency specifically sensitized HSC populations to M-CSF-induced cell division, specific upregulation of the early myeloid selector gene *PU.1*, and a dramatically enhanced myeloid-specific repopulation activity that does not affect self-renewal or differentiation into other lineages. Our results point to a role for MafB in the maintenance of a balanced lineage potential of HSCs by selectively restricting myeloid commitment divisions that give rise to PU.1$^+$ progenitors in response to M-CSF signaling. Together, these data suggest that the potential of stem cells to produce differentiated progeny of a specific lineage bias can be subject to control by integrated cytokine/transcription factor circuits, where variation in cell-intrinsic sensitivity limits like those set by MafB can render external cues such as M-CSF instructive.

RESULTS

Myeloid Lineage-Specific Repopulation Advantage of MafB$^{-/-}$ HSCs

Hematopoietic transcription factors with established roles in mature myeloid cells can have important functions in HSCs (Iwasaki and Akashi, 2007; Orford and Scadden, 2008; Orkin and Zon, 2008; Zon, 2008). Here, we found significant expression of the monocyte/macrophage transcription factor MafB in the highly LT-HSC-enriched CD34$^-$Flt3/Flk2$^-$ population of the primitive c-kit$^+$,sca$^+$,lin$^-$ (KSL) bone marrow fraction but not in downstream progenitors such as in Flt3$^+$KSL multipotent progenitors (MPPs) or in committed common myeloid (CMPs) and granulocyte macrophage (GMPs) progenitors (Figures S1A and S1B available online). Since MafB can influence cellular proliferation in other systems and cell-cycle status is an important determinant of stem cell activity, we further investigated the effect of MafB deficiency on HSC proliferation. Cell-cycle analysis consistently revealed an increased rate of cell division for *MafB*$^{-/-}$ cells in highly LT-HSC-enriched populations as defined by two different stringent marker combinations (CD150$^+$ or CD34$^-$ cells in the Flt3$^-$ KSL [KSLF] fraction) but not in other KSL fractions (Figures 1A, 1B, S1C, and S1D). When we further analyzed the consequence of increased HSC proliferation on stem cell activity in competitive reconstitution assays, we observed a significant advantage of *MafB*$^{-/-}$ but not WT HSCs over normal competitors that resulted in an increased contribution of *MafB*$^{-/-}$ cells to the KSL fraction (Figure 1C). Surprisingly, this competitive advantage of *MafB*$^{-/-}$ HSCs differentially affected the repopulation of lymphomyeloid progeny and resulted in striking differences in the contribution to the different lineages of the hematopoietic system. Twelve weeks after reconstitution, myeloid Mac1$^+$ cells in spleen and bone marrow were largely derived from *MafB*$^{-/-}$ donor cells with a 3-fold and 11-fold excess over WT competitors, respectively (Figure 1D). This competitive advantage was maintained long term in the KSL fraction (Figures S2A and SB) and in mature myeloid cells, including F4/80$^+$ macrophages (Figure 1D). Interestingly, however, the repopulation advantage was lineage specific and not observed in lymphoid or erythroid cells. In peripheral lymphoid organs or bone marrow, the original ratio of donor to competitor was maintained in T cells and only slightly increased in B cells (Figure 1D). Since erythroid cells only weakly express the Ly5 surface marker, we analyzed *MafB*$^{-/-}$ donor contribution to Ter119$^+$ erythroid cells in the bone marrow by quantitative genomic PCR. Quantitative PCR of nonfunctional GFP sequences that specifically tag the *MafB* knockout allele (Blanchi et al., 2003) revealed a linear standard curve for defined mixtures of WT and *MafB*$^{-/-}$ cells (Figures 1E and 1F) and a consistent advantage of *MafB*$^{-/-}$ donor cell contribution to Mac-1$^+$ cells but a contribution to the erythroid lineage that reflected the original injected donor to competitor ratio (Figure 1G).

Despite this strong myeloid-biased repopulation advantage, we did not observe an abnormal increase of total KSL (Figures S2C and S2D) or myeloid cells, myeloproliferative disorders, or leukemia (Figure S3), indicating that *MafB*$^{-/-}$ HSCs outcompeted WT cells in the generation of myeloid progeny without transgressing compartment limits.

To further define the efficiency and kinetics of the myeloid specific repopulation advantage, we followed the contribution of *MafB*$^{-/-}$ HSCs to blood leukocytes of mice reconstituted in excess of competitor cells. Whereas at all dilutions *MafB*$^{-/-}$ stem cells continued to stably contribute to T cells at the initially injected ratio over the whole observation period, we observed a progressively increasing contribution of *MafB*$^{-/-}$ Ly5.2 but not WT Ly5.2 cells to myeloid Mac-1-positive leukocytes even at a 10-fold or 50-fold excess of competitor cells (Figure 2A). This became first observable between 4 and 6 weeks after reconstitution, when originally coinjected progenitors have exhausted their life span and peripheral blood cells will be mainly derived from donor stem cells. At 15 weeks after reconstitution with equal initial input, *MafB*$^{-/-}$ cells had almost entirely outcompeted the WT cells, and in the case of a 10-fold initial competitor excess still provided most cells in the Mac-1-positive population.

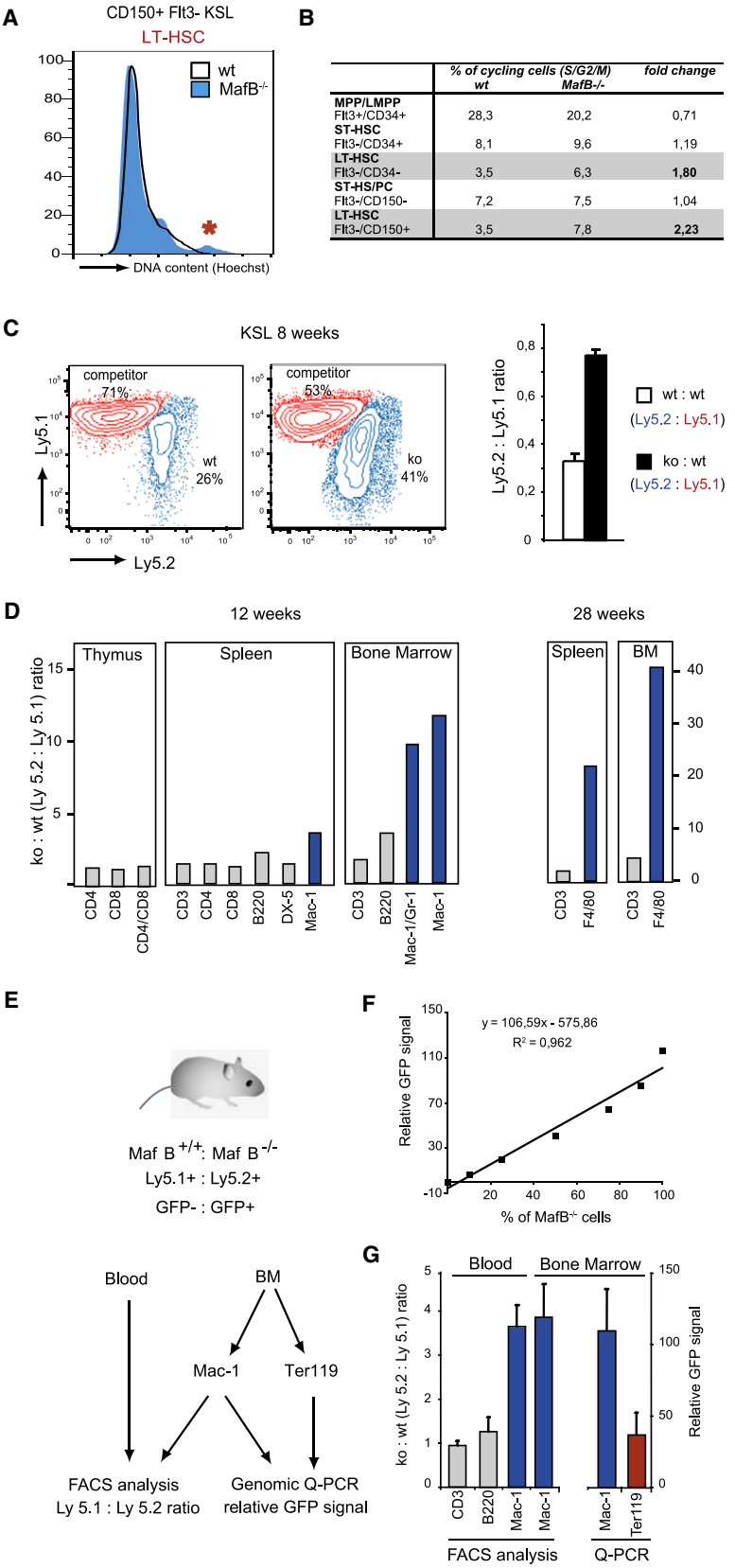

	% of cycling cells (S/G2/M) wt	% of cycling cells (S/G2/M) MafB-/-	fold change
MPP/LMPP Flt3+/CD34+	28,3	20,2	0,71
ST-HSC Flt3-/CD34+	8,1	9,6	1,19
LT-HSC Flt3-/CD34-	3,5	6,3	**1,80**
ST-HS/PC Flt3-/CD150-	7,2	7,5	1,04
LT-HSC Flt3-/CD150+	3,5	7,8	**2,23**

Figure 1. Increased Proliferation and Myeloid Repopulation Bias of *MafB*$^{-/-}$ HSCs

(A) DNA content of highly LT-HSC-enriched bone marrow CD150^{+} KSLF cells.

(B) Percent cells in S/G2/M of different KSL populations (from profiles in A and Figures S1C and S1D).

(C) Contribution of WT or *MafB*$^{-/-}$ (KO) Ly5.2 donor (blue) and WT Ly5.1 competitor cells (red) to the KSL population 8 weeks after transplantation with 3-fold excess of competitor (left) and average donor to competitor ratios (right, n = 4).

(D) Contribution of *MafB*$^{-/-}$ (KO) Ly5.2 cells to different mature lymphoid and myeloid populations showing KO:WT competitor cell ratio (Ly5.2:Ly5.1) of pooled samples 12 weeks (n = 4) or 28 weeks (n = 5) after reconstitution with a mutant to competitor input ratio of 1/1 or 2/1, respectively.

(E) Flow chart of combined FACS and genomic qPCR analysis of mutant allele-specific GFP sequences for *MafB*$^{-/-}$ cell contribution to lymphoid, myeloid, and erythroid cells.

(F) Standard curve of genomic qPCR for defined mixtures of *MafB*$^{-/-}$ and WT bone marrow.

(G) Contribution of *MafB*$^{-/-}$ (KO) Ly5.2 cells to lymphoid, myeloid, and erythroid populations in blood and bone marrow 13 weeks after reconstitution at a mutant to competitor ratio of 1/1 by FACS or genomic qPCR analysis (n = 3).

Error bars indicate the standard error of the mean.

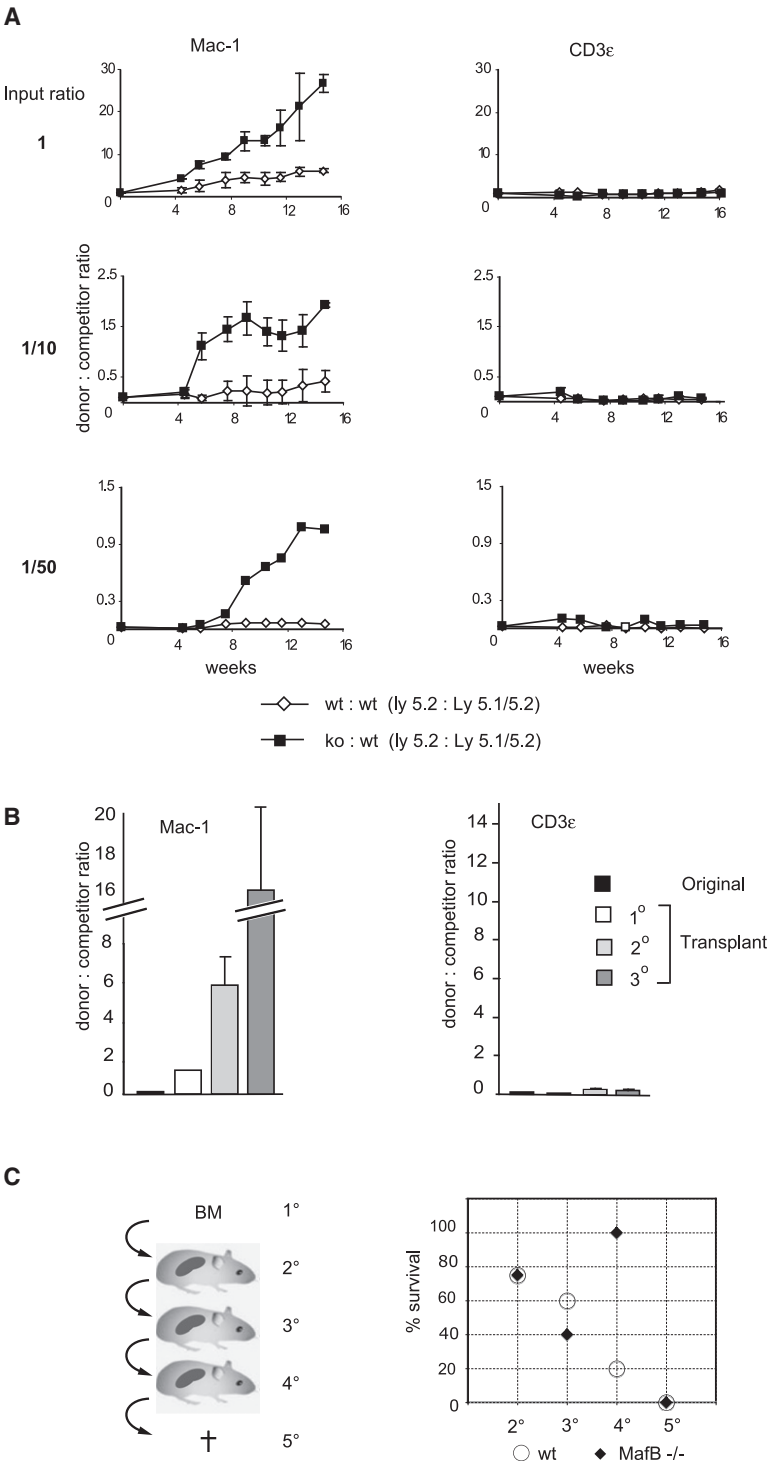

Figure 2. Kinetics and Serial Transplantation of Myeloid Repopulation Bias of *MafB*$^{-/-}$ HSCs

(A) Ly5.1 mice were reconstituted at the indicated input ratios of *MafB*$^{-/-}$ (KO) or WT control Ly5.2 to WT Ly5.1/Ly5.2 (F1) competitor cells. Host, donor, and competitor contribution to Mac-1^{+} myeloid and control CD3ε^{+} lymphoid blood cells were analyzed by FACS (representative profile in Figure S4) and plotted as donor to competitor cell ratio (n = 4 for 1/1 and 1/10).

(B) Donor to competitor ratios in myeloid and T lymphoid blood cells 6 weeks after total bone marrow transplantation from a primary reconstituted mouse with an original 1/10 KO:WT ratio into secondary (at 23 weeks, n = 10) and tertiary (at 25 weeks, n = 5) recipients.

(C) Survival rates from serial transplantation of WT and *MafB*$^{-/-}$ day 12 CFU-S (n = 5).

Error bars indicate the standard error of the mean.

Strikingly, even at the initial ratio of 1/50, which corresponded to the arithmetic equivalent of ~0.2 to 0.6 *MafB*$^{-/-}$ LT-HSCs (assuming a LT-HSC frequency of 1–3/100,000 cells; Bryder et al. [2006]), one out of four injected mice showed a progressive and principally *MafB*$^{-/-}$ contribution to the myeloid compartment by 15 weeks after reconstitution, whereas the three other mice had no Ly5.2 contribution. Together, these results indicated that even at a vast excess of competitor cells, few, possibly a single, *MafB*$^{-/-}$ stem cells could rapidly and progressively outcompete normal cells in the repopulation of the myeloid compartment but continued to contribute faithfully at original ratios to the development of T cells.

Myeloid-Biased Repopulation through Serial Transplantation

Increased proliferative potential of HSCs is frequently associated with stem cell exhaustion and eventual hematopoietic failure of bone marrow transplants (Orford and Scadden, 2008). To determine whether this was the case for *MafB*$^{-/-}$ HSCs, we investigated whether a myeloid selective repopulation advantage could be sustained through serial transplantations. As shown in Figure 2B, serial bone marrow transfer from mice originally reconstituted with a 10-fold excess of competitor cells into secondary and tertiary hosts resulted in continued lymphohematopoietic reconstitution for a cumulative period of over one year and a progressively increasing contribution of *MafB*$^{-/-}$ HSCs to the myeloid compartment. By contrast, *MafB*$^{-/-}$ HSCs continued to faithfully contribute to the T cell lineage at the originally injected ratio. Furthermore, self-renewal was not abnormally increased, as serial transplantation did not affect the total number of KSL cells in the bone marrow (Figure S5). Repeated transfer of CFU-S12 colonies from competitive WT or *MafB*$^{-/-}$ reconstitutions also showed complete hematopoietic failure and death of recipients after the fifth transplantation (Figure 2C), as expected from previous reports (Siminovitch et al., 1964). Taken together, our results indicate that *MafB*$^{-/-}$ HSCs neither abnormally exhaust nor increase their self-renewal capacity, continue to contribute to all lineages, and sustain a progressively increasing myeloid repopulation advantage through serial transplantation.

MafB Deficiency Confers a Specific Advantage in Generating Myeloid Progeny in Culture

We next investigated whether the myeloid-specific repopulation advantage of *MafB*$^{-/-}$ HSCs was cell intrinsic and was reflected in increased generation of myeloid progeny in culture. Toward this end, we cultured sorted KSL cells under myeloid differentiation conditions in SCF, TPO, and M-CSF (Iwama et al., 2004) or in the presence of Flt-3 ligand and Il-7 on OP9-DL1 cells, which support T cell differentiation from HSC populations (Schmitt and Zuniga-Pflucker, 2002). Cell counts at 24 hr intervals revealed that after 4.5 days under myeloid conditions, *MafB*$^{-/-}$ cells had generated significantly more progeny cells than their WT counterparts (Figure 3A). By contrast, *MafB*$^{-/-}$ cells showed no difference from WT cells under lymphoid differentiation conditions (Figure 3B). Notably, the increased cell production under myeloid conditions did not prevent differentiation or change the final phenotype of differentiated cells, as judged by a similar Mac-1/Gr-1 or CD25/CD44 expression profile after 5 days of myeloid or T cell differentiation conditions, respectively (Figures 3A and 3B). Furthermore, increased generation of myeloid progeny from *MafB*$^{-/-}$ KSL cells depended on an increased response to myeloid conditions during the initial culture period (Figure 3C), whereas myeloid-committed CMPs responded well but showed no difference between WT and *MafB*$^{-/-}$ samples (Figure 3D). Consistent with this and in contrast to KSL cell controls, purified sca^{-}, ckit^{+} progenitors that include CMP also couldn't initiate a myeloid specific repopulation advantage in vivo (Figure S6). Together, these observations indicated that the increased proliferation and myeloid specific repopulation advantage of *MafB*$^{-/-}$ HSCs corresponded to an intrinsic capacity to specifically generate more myeloid progeny in culture.

MafB Specifically Limits Sensitivity to M-CSF Signaling

The ability of *MafB*$^{-/-}$ KSL cells to generate more myeloid progeny was only observed in the presence but not in the absence of M-CSF (Figure 3C). Furthermore, other myeloid cytokines such as GM-CSF, Il-3, and G-CSF or FGF, a cytokine with profound effects on HSCs (Zhang and Lodish, 2008) that acts through a similar receptor tyrosine kinase as M-CSF, also had no differential effect (Figure 3E). When we further investigated this M-CSF response in vivo by cell-cycle analysis 16 hr after direct injection of recombinant M-CSF into the blood stream of WT or MafB$^{-/-}$ reconstituted mice, we also observed a significant increase in the cycling fraction of *MafB*$^{-/-}$ KSL cells but not of c-kit^{+}sca^{-} progenitors (Figures 3F and 3G).

This enhanced M-CSF-specific response could depend on increased M-CSF receptor (M-CSFR) expression, increased cellular sensitivity to M-CSFR signaling, or both. Although we observed a small increase of M-CSFR message levels both in total KSL and HSC-enriched KSLF cells (Figures S7A and S7B), this effect appeared to be too small to account for the observed phenotype and may simply occur as a secondary effect of higher sensitivity to receptor signaling, since the expression of M-CSFR is under positive feedback control from its own signals (Xie et al., 2001). To uncouple M-CSFR signaling from regulation of its promoter, we therefore infected WT or *MafB*$^{-/-}$ cyclophosphamide-mobilized stem/precursor cells with a td-tomato retrovirus expressing a constitutively active form of M-CSFR (M-CSFR*), whose signaling and expression is independent of exogenous M-CSF (Carlberg and Rohrschneider, 1994). After 36 hr in culture, we observed a significant increase of cycling cells (S/G2/M) in M-CSFR* over control virus infected *MafB*$^{-/-}$ KSL cells but not in WT KSL cells or in the uninfected td-tomato^{-} population (Figures 4A and 4B). To further test whether conversely, ectopic MafB expression could specifically restrict M-CSFR dependent myeloid divisions under conditions of uncoupled receptor expression and signaling, we used a conditionally transformed T lymphoid cell line that ectopically expresses M-CSFR from a heterologous, M-CSF-independent promoter and does not express endogenous MafB or M-CSFR (EGER-fms; Bourette et al. [2007]). After infection with a MafB-GFP or GFP control retrovirus, we cultured this cell line alternatively under myeloid or lymphoid conditions in M-CSF or Il-7/SCF, respectively. BrdU incorporation and cell-cycle analysis revealed that MafB almost completely inhibited M-CSF-dependent cell division, but had no effect on cell-cycle progression under lymphoid conditions (Figures 4C and 4D). Thus, both gain- and loss-of-function experiments in multipotent cells revealed that MafB can selectively limit sensitivity to M-CSFR signaling.

To further test whether increased sensitivity to endogenous M-CSF signaling was at the basis of the myeloid-specific repopulation advantage of *MafB*$^{-/-}$ HSCs in vivo, we generated a GFP retrovirus expressing short hairpin RNA (shRNA) directed against the M-CSFR (shFms), which was highly effective in reducing its surface expression (Figure 4E). We infected *MafB*$^{-/-}$ Ly5.2 fetal liver cells with shFms virus, injected them together with F1 competitor cells into lethally irradiated Ly5.1 recipients, and analyzed the effect on competitive repopulation in the spleen, where a myeloid-specific advantage of *MafB*$^{-/-}$ HSCs could already be detected 12 days after reconstitution (Figure S8). Comparison of GFP^{+} and GFP^{-} populations in the Mac-1^{+} and Mac-1^{-} fraction of shFms virus-infected donor cells revealed that reduction of M-CSFR levels decreased the myeloid-specific repopulation advantage of *MafB*$^{-/-}$ cells (Figure 4F), whereas a control virus had no such effect (data not shown). Together, these results indicated that *MafB*$^{-/-}$ HSCs are sensitized to M-CSF-driven myeloid repopulation in vivo.

MafB Limits M-CSF Instructed Myeloid Commitment

To further test whether higher M-CSF sensitivity specifically resulted in increased myeloid commitment divisions of *MafB*$^{-/-}$ HSCs, we analyzed M-CSF-dependent activation of PU.1, a myeloid master regulator that is both required for and sufficient to drive myeloid fate (Iwasaki and Akashi, 2007) and is important for the initial steps of differentiation, as myeloid precommitted PU.1^{+} progenitors (PU.1^{+} MPPs) can already be detected in the Flt3^{+} fraction of KSL cells (Arinobu et al., 2007). Quantitative RT-PCR revealed that PU.1 was expressed only at very low levels in *MafB*$^{-/-}$ or WT cells of the HSC-enriched KSLF population but increased dramatically in *MafB*$^{-/-}$ cells after 16 hr of M-CSF stimulation (Figure 5A). Immunofluorescence also confirmed an increase in PU.1 protein levels and the number of PU.1^{+} cells (Figure 5B). By contrast, M-CSF-stimulated *MafB*$^{-/-}$ cells showed no change or reduced expression levels of erythroid and lymphoid lineage transcription factors (Figure 5C).

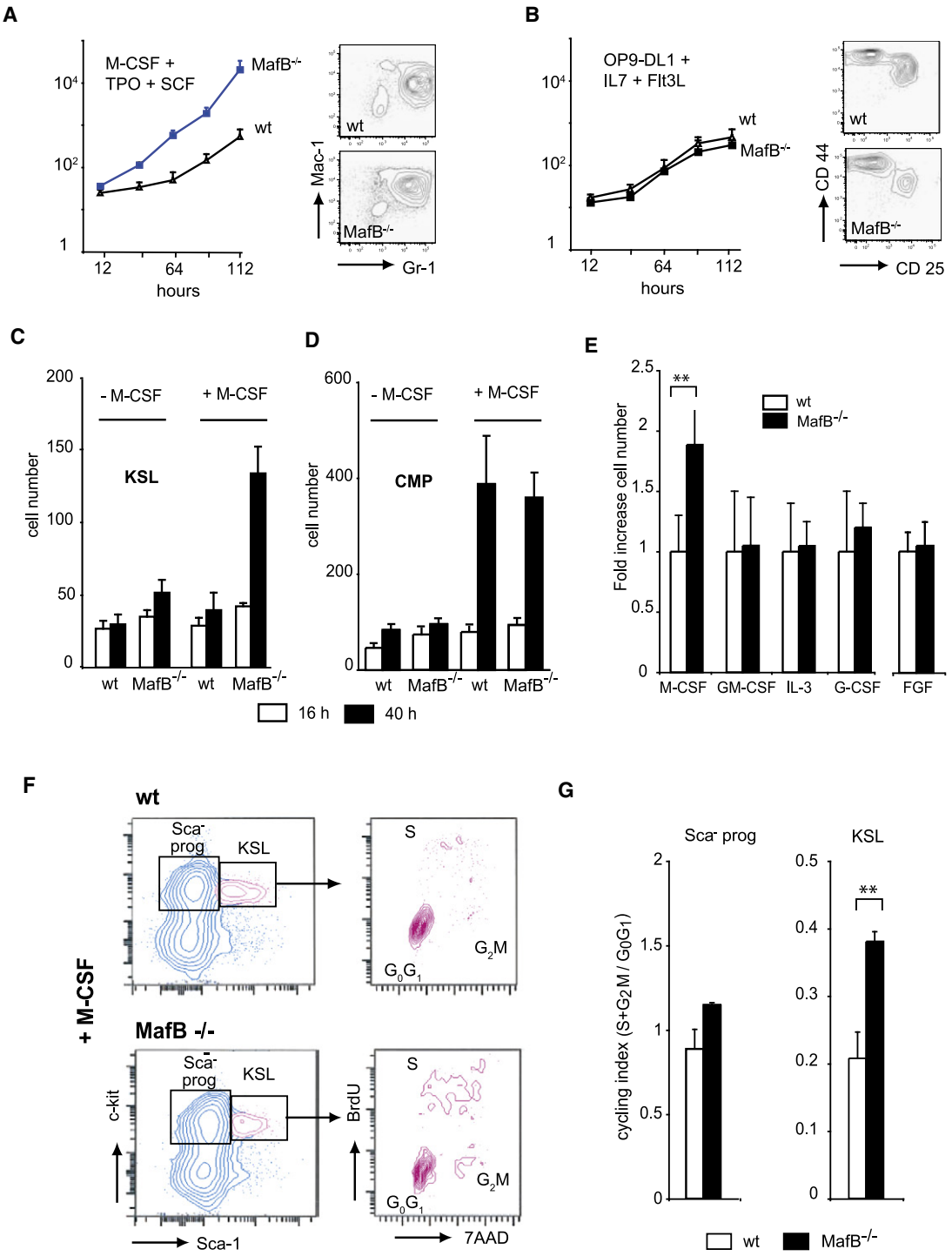

Figure 3. Myeloid-Specific Growth Advantage Is Cell Intrinsic and M-CSF Dependent

(A and B) Cumulative cell counts of FACS-sorted KSL cells (n = 6) under myeloid (A) or T cell differentiation (B) conditions and Mac-1/Gr-1 or CD44/CD25 profile on day 5.

(C and D) FACS-sorted KSL (C) or CMP (D) cells (n = 6) were cultured in the absence or presence of M-CSF and counted after 16 hr and 40 hr.

(E) Fold increase in cell number of *MafB*$^{-/-}$ over WT cells after 40 hr culture of 60 FACS-sorted KSL cells with M-CSF, GM-CSF, Il-3, G-CSF, or FGF.

(F and G) Cell-cycle analysis showing BrdU/7-AAD profiles (F) and cycling indices (S/G2/M to G0/G1) (G) of bone marrow KSL cells (pink) and sca^{-} progenitors 16 hr after IV injection of 5 μg rM-CSF. **p < 0.01 by two-tailed Mann-Whitney test.

Error bars indicate the standard error of the mean.

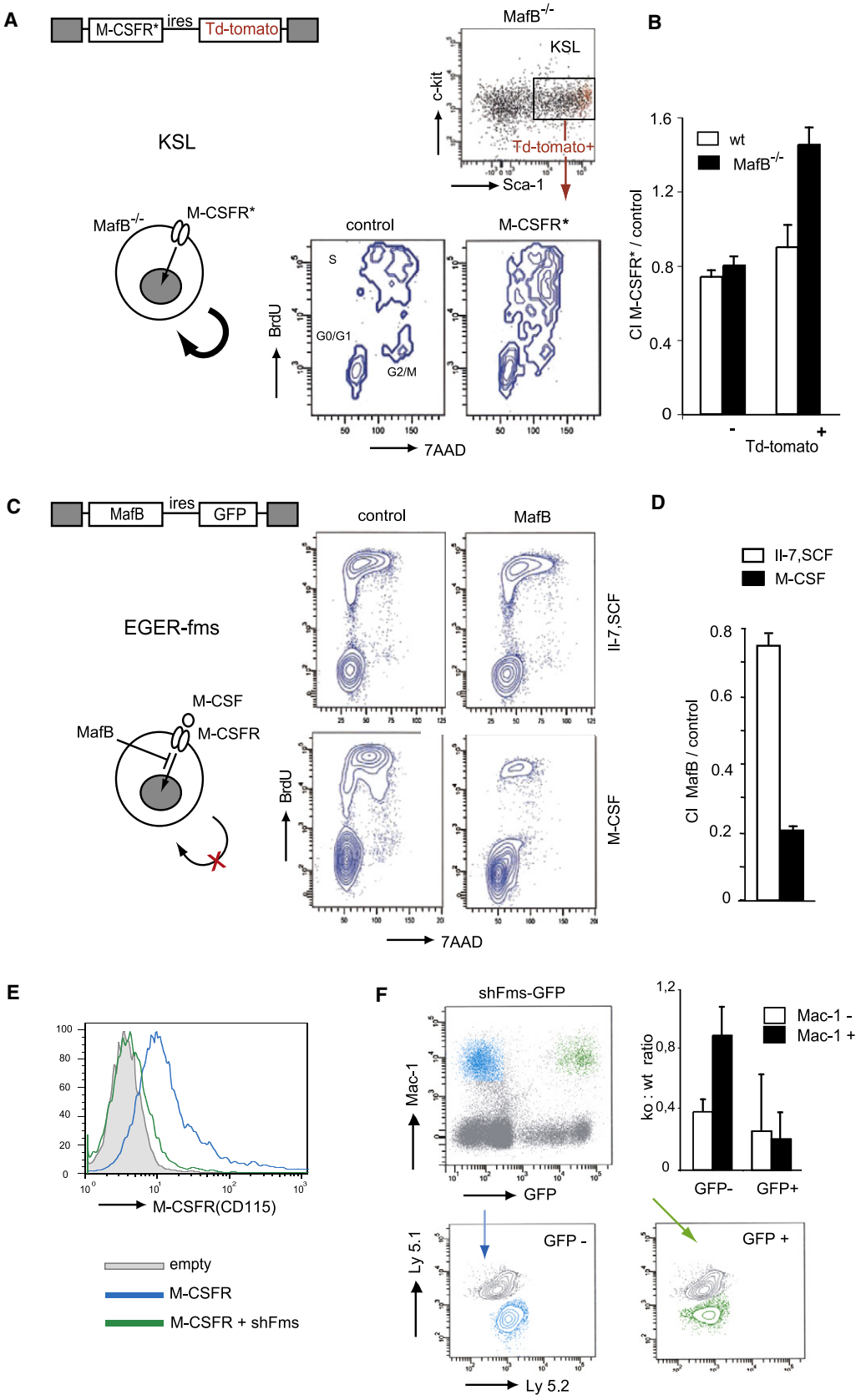
A
M-CSFR*
ires
Td-tomato
KSL
MafB-/-
M-CSFR*
MafB-/-
KSL
c-kit
Sca-1
Td-tomato+
control
M-CSFR*
S
G0/G1
G2/M
BrdU
7AAD
B
wt
MafB-/-
CI M-CSFR* / control
1.6
1.2
0.8
0.4
0
-
+
Td-tomato
C
MafB
ires
GFP
EGER-fms
M-CSF
MafB
M-CSFR
control
MafB
Il-7,SCF
M-CSF
BrdU
7AAD
D
Il-7,SCF
M-CSF
CI MafB / control
0.8
0.6
0.4
0.2
0
E
M-CSFR(CD115)
empty
M-CSFR
M-CSFR + shFms
F
shFms-GFP
Mac-1
GFP
Ly 5.1
Ly 5.2
GFP -
GFP +
Mac-1 -
Mac-1 +
ko : wt ratio
GFP-
GFP+

This indicated that MafB deficiency specifically enabled M-CSF-dependent activation of the early myeloid commitment factor PU.1.

To further characterize M-CSF-dependent myeloid commitment divisions, we made use of *PU.1*-GFP reporter mice that make it possible to clearly distinguish PU.1$^-$ Flt3$^-$ HSC and precursor populations (PU.1$^-$ KLSF) from precommitted PU.1$^+$ Flt3$^+$ progenitors (PU.1$^+$ MPPs) within the KSL fraction (Arinobu et al., 2007). As shown in Figure 6A, MafB was highly expressed in the PU.1$^-$ KLSF fraction but not in PU.1$^+$ MPPs, suggesting that development of such progenitors from HSCs requires MafB downregulation. To test whether reduced MafB levels could thus facilitate M-CSF-induced generation of PU.1$^+$ MPPs from PU.1$^-$ KLSF cells, we crossed the *MafB* knockout allele on the *PU.1*-GFP reporter background and sorted PU.1$^-$ KSLF cells (population A in Figure 6A) from heterozygous *MafB*$^{+/-}$ *PU.1*-GFP or WT *PU.1*-GFP fetal livers (*MafB*$^{-/-}$ *PU.1*-GFP embryos not being viable). As shown in Figure 6B, 20 hr stimulation with M-CSF but not with Il-3 resulted in increased PU.1$^+$ cells in *MafB*$^{+/-}$ samples. Since HSCs and precursor cells do not divide more than once during this time (Wu et al. [2007]; S.S. and M.H.S., unpublished data) the development of PU.1$^+$ progenitors from PU.1$^-$ KLSF cells demonstrated that reduced MafB dosage specifically enables M-CSF-stimulated myeloid commitment divisions in PU.1$^-$ KSLF cells. To further confirm this, we sorted PU.1$^-$ KSLF cells directly into 384-well plates and revisited single cells by microscopy until their first division and monitored the activation of the *PU.1*-GFP reporter in the daughter cells. As shown in Figure 6C, we could detect both divisions giving rise to symmetric PU.1$^-$/PU.1$^-$ and PU.1$^+$/PU.1$^+$ daughter pairs and divisions giving rise to asymmetric PU.1$^-$/PU.1$^+$ daughter pairs. Significantly, reduced MafB dosage selectively increased the development of mixed PU.1$^-$/PU.1$^+$ daughter pairs, indicating that MafB deficiency specifically enhanced M-CSF-driven asymmetric myeloid commitment divisions of KLSF stem and precursor cell populations.

To further confirm that MafB deficiency also enabled increased myeloid commitment of highly enriched HSC populations in vivo, we FACS sorted CD150$^+$ KSLF cells, labeled them with CSFE, and directly injected them into the spleen of irradiated hosts (Figure 7A), a hematopoietic organ that provides appropriate stem cell niches for extra-medullary hematopoiesis after HSC mobilization or transplantation (Kiel and Morrison, 2008). In spleens recovered 24 hr after transplantation, we could clearly detect CFSE$^+$ cells and unambiguously distinguish PU.1-expressing and PU.1-negative cells by anti-PU.1 immunofluorescence (Figure 7B). Sectioning of the whole organ and analysis of every other section recovered about 1%–2% of injected donor cells, but whereas only a small proportion of WT cells were found to express PU.1, a large majority of *MafB*$^{-/-}$ cells was PU.1 positive (Figures 7C and 7D). Together, these data demonstrated that MafB deficiency also enabled increased commitment of highly purified HSCs to PU.1$^+$ cells in a normal hematopoietic environment in vivo.

To finally test whether PU.1 activation was required for the myeloid repopulation advantage of *MafB*$^{-/-}$ HSCs in vivo, we generated several GFP retroviruses expressing shRNA directed against PU.1, one of which was highly effective in reducing PU.1 levels (shPU.1/3; Figure 6D). We infected *MafB*$^{-/-}$ Ly5.2 fetal liver cells with shPU.1/3, injected them together with F1 competitor cells into lethally irradiated Ly5.1 recipients, and analyzed the effect on competitive repopulation in the spleen as described above (Figures S8 and 4F). Comparison of GFP$^+$ and GFP$^-$ populations in the Mac-1$^+$ and Mac-1$^-$ fraction of shPU.1 virus-infected donor cells revealed that reduction of PU.1 levels decreased the myeloid-specific repopulation advantage of *MafB*$^{-/-}$ cells (Figure 6E). These results further indicated that PU.1 activation is required for the myeloid repopulation advantage of *MafB*$^{-/-}$ HSCs in vivo.

DISCUSSION

Here, we reported that MafB activity restricts M-CSF-induced myeloid commitment divisions of HSCs. Our data support a direct instructive effect of M-CSF on HSCs rather than a permissive action on the amplification of down stream progenitors.

The primitive KSL fraction of the bone marrow contains, besides LT-HSCs in the CD34$^-$/Flt-3$^-$ compartment, CD34$^+$ and Flt3$^+$ MPPs, which not only have a more limited self-renewal potential (Bryder et al., 2006) but can also exhibit different lineage bias (Iwasaki and Akashi, 2007; Luc et al., 2008), in particular the mutually exclusive GATA-1$^+$ and PU.1$^+$ subpopulations of the CD34$^+$ KSL fraction that are precommitted to distinct lineages (Arinobu et al., 2007). Several results indicate that MafB restricts M-CSF-dependent commitment of HSCs to PU.1$^+$ MPPs rather than M-CSF-dependent amplification of such progenitors after their generation. First, MafB is expressed in immunophenotypic HSCs (CD34$^-$ Flt3$^-$ KSL) but not in PU.1$^+$ MPPs. Furthermore, we observed increased proliferation of *MafB*$^{-/-}$ HSCs using two stringent immunophenotypic

Figure 4. MafB Specifically Restricts Sensitivity to M-CSF Signaling

(A) Cyclophosphamide-mobilized stem and precursor cells from *MafB*$^{-/-}$ bone marrow were infected with a td-tomato control virus or a retrovirus expressing a constitutively active M-CSFR (M-CSFR*) to analyze cell-cycle profiles of td-tomato$^+$ cells in the KSL fraction after 36 hr culture without M-CSF.

(B) Ratio of the cycling index (S/G2/M to G0/G1) for M-CSFR* to control virus infected cells, for the td-tomato$^+$ and td-tomato$^-$ fraction of WT and *MafB*$^{-/-}$ KSL samples (n = 2) as shown in (A).

(C) EGER-fms T cells that ectopically express M-CSFR were infected with MafB-GFP retrovirus or GFP control virus to analyze the cell-cycle profiles of GFP$^+$ cells after 6 hr culture in T cell (SCF, IL-7) or M-CSF conditions.

(D) Ratio of the cycling index (S/G2/M to G0/G1) for MafB to control virus infected cells under T cell and M-CSF conditions as shown in (C) (n = 2).

(E) M-CSFR cell surface expression on HEK293 cells cotransfected with M-CSFR expression vector and anti-M-CSFR shRNA (shFms) or empty control vector.

(F) Analysis of spleen 11 days after transplantation of Ly 5.1 recipients with shFms-GFP retrovirus infected *MafB*$^{-/-}$ (KO) Ly 5.2 fetal liver cells and WT F1 competitor cells. Representative FACS profiles of KO donor and WT competitor contribution to Mac-1$^+$ myeloid cells in GFP$^-$ (blue) or shFms-GFP infected GFP$^+$ populations (green) and quantification of KO:WT ratios in GFP$^-$ and GFP$^+$ populations of Mac-1$^+$ and Mac-1$^-$ spleen cells (n = 4).

Error bars indicate the standard error of the mean.

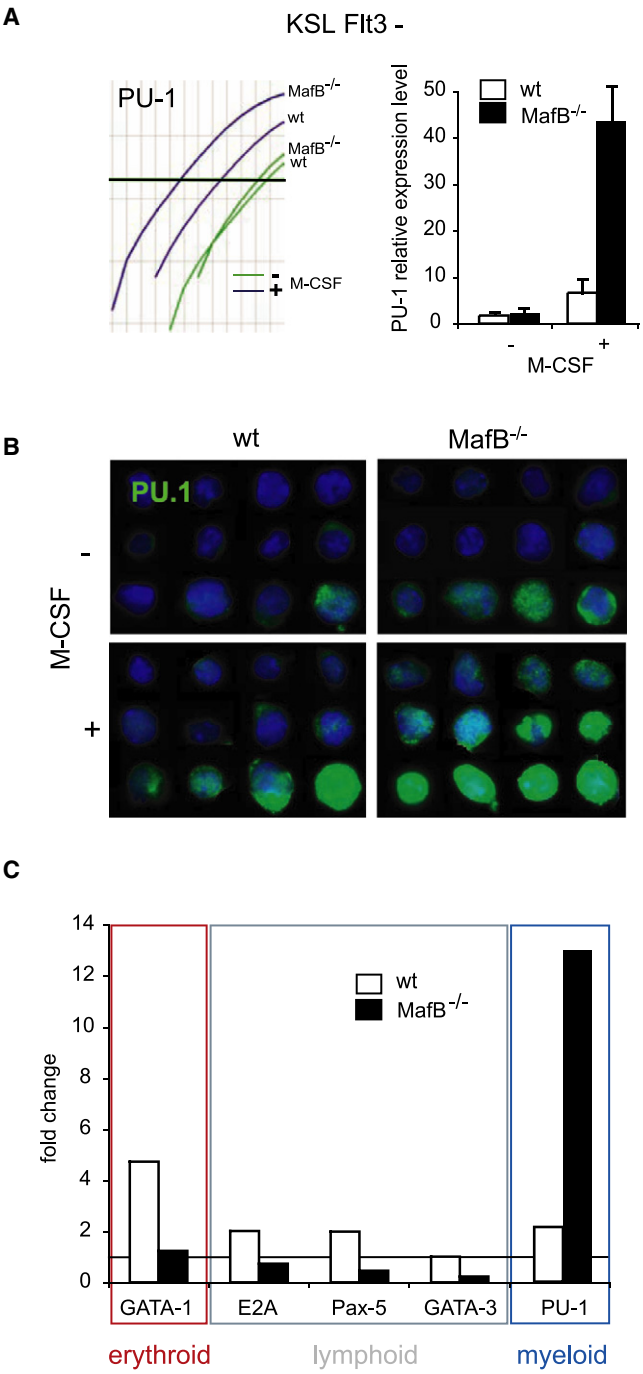

Figure 5. MafB Deficiency Enables M-CSF-Dependent *PU.1* Activation

(A) Analysis of relative PU.1 message levels by qRT-PCR in KSLF cells before and after 16 hr incubation with 100 ng/ml M-CSF, showing primary Ct and HPRT normalized values.

(B) Analysis of PU.1 protein expression by immunofluorescence on KSLF cells before and after 6 hr incubation with 100 ng/ml M-CSF. Assembled image of randomly chosen cells.

(C) Fold changes of lineage-specific transcription factor expression in KSLF cells after culture with M-CSF, measured by qRT-PCR under the same conditions as in (A).

Error bars indicate the standard error of the mean.

definitions ($CD34^-$ $Flt3^-$ KSL or $CD150^+$ $Flt3^-$ KSL) but not in any of the $CD150^-$, $CD34^+$, or $Flt3^+$ MPP populations, which would be expected to show increased cycling in a permissive mechanism that depends on the amplification of progenitors after commitment. Since in addition *MafB*$^{-/-}$ HSCs showed a myeloid-specific repopulation advantage without expansion of the stem cell pool, this is highly consistent with increased commitment divisions of HSCs. Furthermore, reduced MafB dosage specifically enabled M-CSF-dependent generation of $PU.1^+$ daughter cells from individual $PU.1^-$ KSLF cells during the first cell division. Since these cells were PU.1 negative before exposure to M-CSF and were only analyzed for one cell division, this experiment excluded selection of pre-existing $PU.1^+$ cells or the amplification of $PU.1^+$ daughter cells after a stochastic commitment event. Finally, MafB deficiency increased myeloid commitment not only in KSLF cells (that also contain ST-HSCs) in culture but also in individual $CD150^+$ KSLF cells in vivo. Transplantation of these highly LT-HSC-enriched cells into the spleen, a hematopoietic organ that provides appropriate stem cell niches (Kiel and Morrison, 2008), showed a dramatically increased commitment to $PU.1^+$ cells within 24 hr, a time period during which the vast majority of transplanted and similarly defined HSC populations do not undergo more than one division (Lo Celso et al., 2009). Together, our data thus indicate that MafB deficiency enables M-CSF to instruct myeloid commitment divisions in HSCs that generate increased $PU.1^+$ MPPs.

Interestingly, $PU.1^+$ MPPs can directly give rise to GMPs without passing through a CMP stage (Arinobu et al., 2007), which may explain the selectively myeloid-biased repopulation advantage of *MafB*$^{-/-}$ HSCs in the absence of effects on the erythroid lineage. In contrast to the complete absence of any effect on the T cell lineage and in addition to the strong myeloid advantage, we also observed a slight and delayed advantage of *MafB*$^{-/-}$ HSCs in reconstituting the B cell compartment (Figure 1 and data not shown). This is consistent with the ability of PU.1 to also instruct B cell fate at lower expression levels (DeKoter and Singh, 2000).

HSC division can result in self-renewal or differentiation, but the mechanisms controlling the different outcomes of a HSC division remain unresolved. Several mutant mice with a HSC-cycling phenotype have been characterized, but so far were exclusively found to affect self-renewal (Orford and Scadden, 2008). Here, we show that by contrast the higher proliferation rate of *MafB*$^{-/-}$ HSCs appears to be dedicated to increased myeloid commitment divisions. Consistent with this, MafB deficiency did not result in abnormal expansion of the stem cell pool or myeloproliferative disorders. Furthermore, it did not cause stem cell depletion or compromise differentiation to other lineages, suggesting that augmented myeloid commitment divisions occur in addition rather than at the expense of other HSC divisions.

Evidence from both invertebrate and mammalian models indicates that stem cells can undergo both asymmetric divisions that give rise to mixed stem and differentiated daughter cell pairs (S/D) and symmetric divisions with two stem cell daughter pairs (S/S) or two differentiated cell daughter pairs (D/D) (Knoblich, 2008; Morrison and Kimble, 2006). Moreover, hematopoietic stem and precursor cells in culture can change the relative proportion of asymmetric divisions in response to external

cues such as cytokines or stromal cells (Takano et al., 2004; Wu et al., 2007). Although we cannot exclude that on a population basis in vivo, S/S division-buffered myeloid D/D type divisions also contribute to increased myeloid commitment, our single-cell experiments show that reduced MafB levels specifically increased M-CSF-stimulated asymmetric divisions, giving rise to PU.1^{-}/PU.1^{+} daughter pairs. This observation provides a conclusive explanation as to why increased myeloid commitment of *MafB*$^{-/-}$ HSCs does not come at the expense of self-renewal or other lineages, since asymmetric stem cell divisions do not change the total number of stem cells and thus maintain a stable stem cell pool that remains available for subsequent self-renewal and generation of other lineages. MafB deficiency therefore appears to enable enhanced myeloid commitment without affecting self-renewal or other lineages by selectively increasing asymmetric myeloid commitment divisions of HSCs.

Although the role of both lineage specific transcription factors and cytokines in HSC commitment has been discussed (Enver et al., 1998; Hu et al., 1997; Metcalf, 2008; Orkin and Zon, 2008; Sieweke and Graf, 1998; Zhang and Lodish, 2008), it is not clear how the two regulatory systems may be integrated. It has been proposed that HSC fate decisions may depend on sensitivity thresholds of cytokine signaling (Zandstra et al., 2000), but whether cytokines could play an instructive role in lineage commitment has remained highly controversial (Enver et al., 1998; Metcalf, 1998). Our results now indicate that lineage-specific transcription factors such as MafB may play a key role in HSCs by setting cytokine sensitivity thresholds and that transcription factor expression below a certain level could render external cues instructive. Such critical variations in expression levels that we induced experimentally may occur naturally through external cues, cell-intrinsic stochastic fluctuation (Chang et al., 2008), or stably inherited epigenetic modifications (Dykstra et al., 2007; Jordan and Lemischka, 1990; Muller-Sieburg et al., 2002). Indeed, by transplantation of individual HSCs, Dykstra et al. have functionally defined a population of so-called α cells with an intrinsically set myeloid lineage bias that can be stably transmitted through serial transplantation. To a certain extent, this resembles the properties of *MafB*$^{-/-}$ HSCs, and it will be interesting to determine whether HSCs can fix a certain differentiation preference by epigenetic repression of cell intrinsic threshold setters such as MafB.

Furthermore, the availability of M-CSF may also play an important role in controlling HSC commitment divisions. Interestingly, in the bone-marrow M-CSF is mainly produced by a subset of osteoblasts and endothelial cells (Ryan et al., 2001) and thus potentially in direct vicinity to endosteal and perivascular stem cell niches (Adams and Scadden, 2006; Kiel and Morrison, 2008; Wilson and Trumpp, 2006). Both cell-intrinsic susceptibility and levels of external cues may thus cooperate to control HSC-specific commitment divisions. We predict that other lineage-specific transcription factors besides MafB may similarly act as threshold setters for other cytokines and thus control the exit of HSCs toward different differentiation pathways. The fine-tuned balance of these factors would thus result in an appropriate response to the available external cues and thus assure both adaptive and stable HSC behavior under different physiological conditions.

EXPERIMENTAL PROCEDURES

Mice, CFU-S Assays, and FACS Analysis

MafB$^{-/-}$ (Blanchi et al., 2003) and *PU.1*-GFP reporter mice (Arinobu et al., 2007) have been described. Age- and sex-matched Ly5.1 or F1 recipients were reconstituted as described (Aziz et al., 2006) with competitor cells from Ly5.1 fetal liver or F1 ACK lysed bone marrow (BM). Macroscopic analysis and serial transplantations of CFU-S was done as described (Siminovitch et al., 1964) by IV injection of lethally irradiated C57BL/6J mice with 4 × 10^{6} BM cells from primary transplants or secondary spleenocyte suspensions. For FACS analysis, we used described staining protocols (Aziz et al., 2006), published stem and progenitor cell definitions (Bryder et al., 2006), FACSCanto, LSRII, and FACSAria equipment and DIVA software (Becton Dickinson).

Cell Culture and Retroviral Infections

EGER-fms pro-T cells were cultured as described (Bourette et al., 2007) under T cell (50 ng/ml rSCF, 10 ng/ml rIL-7, 1 μM β-estradiol [Sigma]) or myeloid conditions (50 ng/ml rM-CSF). KSL cells were sorted into S clone SF-03 medium (Sanko Jyunyaku) with 10% FBS (SCM) and seeded at 60 cells/96-well (uncoated U shape, Greiner) in 100 μl SCM, 20 ng/ml rSCF, 50 ng/ml rTPO ± 100 ng/ml rM-CSF, rG-CSF, rGM-CSF, rIl-3, or human rFGF-a (Biosource) or at 60 cells/96-well in SCM, 5 ng/ml rFlt3-L, 5 ng/ml rIL-7 on irradiated OP9-DL1 stromal cells under the described conditions (Schmitt and Zuniga-Pflucker, 2002). All cytokines were murine and from PeproTech if not otherwise indicated.

MSCV-based retroviral vectors were constructed by PCR cloning complementary DNAs (cDNAs) of murine MafB or an activated M-CSFR mutant (c-fms S301,S374, Δ3′; Carlberg and Rohrschneider [1994]) under LTR control and by replacement of the IRES-driven GFP with td-tomato cDNA (Clontech), to generate MafB-GFP and M-CSFR*-tdTomato. shRNA sequences (Table S1) were determined with RNAi Codex software (http://codex.cshl.edu/scripts/newmain.pl) and cloned into LMP-GFP virus (Open Biosystems). Viral supernatants were produced with ϕNXe cells (http://www.stanford.edu/group/nolan) and used to infect EGER-fms or primary BM cells by a double 2h-spinoculation with 8 μg/ml polybrene. To enrich for cycling KSL cells, BM was harvested 24 hr after IP injection of 600 μl PBS containing 10 mg/ml cyclophosphamide (Sigma). For shFms and shPU.1/3 virus infection, fetal liver cells were cultured 24 hr prior to infection in medium supporting stem cell amplification (IMDM 15% FBS, 100 ng/ml rIl-11, 100 ng/ml rSCF, 50 ng/ml rFlt3L, 10 ng/ml rTPO, 10^{-5} M β-Mercaptoethanol).

Western Blotting, Quantitative Real-Time PCR, and RT-PCR

Western blots were performed as described (Bakri et al., 2005) with anti-PU.1 antibody (Cell signaling, #2258) at 1:1000 dilution. Genomic DNA was extracted with the DNeasy Mini kit (QIAGEN). Total RNA was isolated and reverse transcribed with μMACS One-step T7 Template Kit (Miltenyi Biotec) or extracted with the RNeasy Mini kit (QIAGEN), digested with DNase I (QIAGEN), and reverse transcribed with SuperScript II (Invitrogen). For quantitative real-time PCR, we used Power SYBR Green PCR Master Mix and a 7500 Fast Real Time PCR System sequence detection system (both Applied Biosystem), following the manufacturers' instructions. For primers, see Table S1.

Fluorescence Microscopy

For single daughter pair analysis, PU.1^{-} KSLF cells were directly sorted into conical 384-well glass bottom plates (SensoPlate, Greiner) with 20 μl SCM, 20 ng/ml rSCF, 50 ng/ml rTPO, 100 ng/ml rM-CSF (myeloid SCM). Single cells were revisited until the first division for a maximum of 40 hr, and daughter cells were monitored for GFP expression with a Zeiss Axiovert 200 inverted microscope.

For anti-PU.1 IF, 2 × 10^{3} KSLF cells were seeded in V-shaped 96-well plates (Greiner) in 100 μl myeloid SCM. Cells were fixed before or after culture in myeloid SCM with PBS/2% paraformaldehyde (PFA) for 10 min at room temperature, neutralized in PBS/100 mM glycine, washed 2× in PBS, incubated for 30 min in PBS/2% BSA/2% FCS/2% donkey serum/0.1% saponin (P buffer), 30 min with anti-PU.1 antibody (T-21, sc-352, Santa Cruz) in P buffer

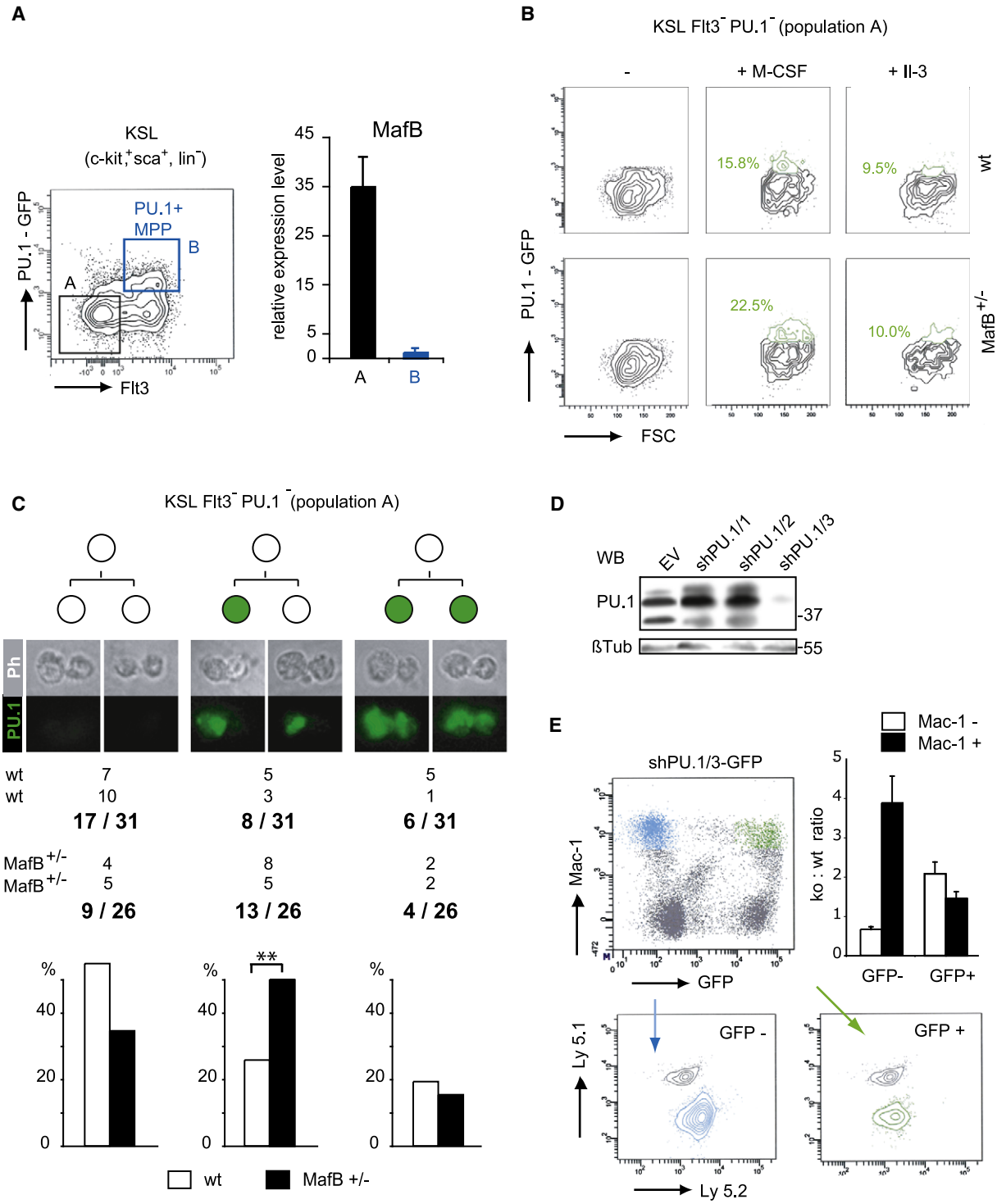

Figure 6. MafB Restricts M-CSF-Instructed Asymmetric Myeloid Commitment Divisions

(A) Relative MafB message levels in HSC-enriched PU.1$^-$ Flt-3$^-$ cells (PU.1$^-$ KSLF, gate A) and PU.1$^+$ Flt-3$^+$ progenitors (PU.1$^+$ MPP, gate B) in the KSL fraction of *PU.1*-GFP reporter mice (HPRT normalized qRT-PCR values).

(B) Representative profiles of *PU.1*-GFP expression in PU.1$^-$ KSLF cells (gate A in panel A) from *MafB*$^{+/-}$ and WT *PU.1*-GFP reporter mice before and after 20 hr incubation with 100 ng/ml M-CSF or Il-3.

(C) PU.1$^-$ KSLF cells (gate A in panel A) of *MafB*$^{+/-}$ and WT *PU.1*-GFP reporter mice were directly sorted into 384-well plates with 100 ng/ml M-CSF containing medium. Single cells were revisited until the first division and daughter cells monitored for GFP expression. Two representative samples each of PU.1$^{-/-}$, PU.1$^{+/-}$ and PU.1$^{+/+}$ daughter pairs, counts from two independent experiments, and proportions of division types are shown. **p = 0.01 by Pearson's Chi square test.

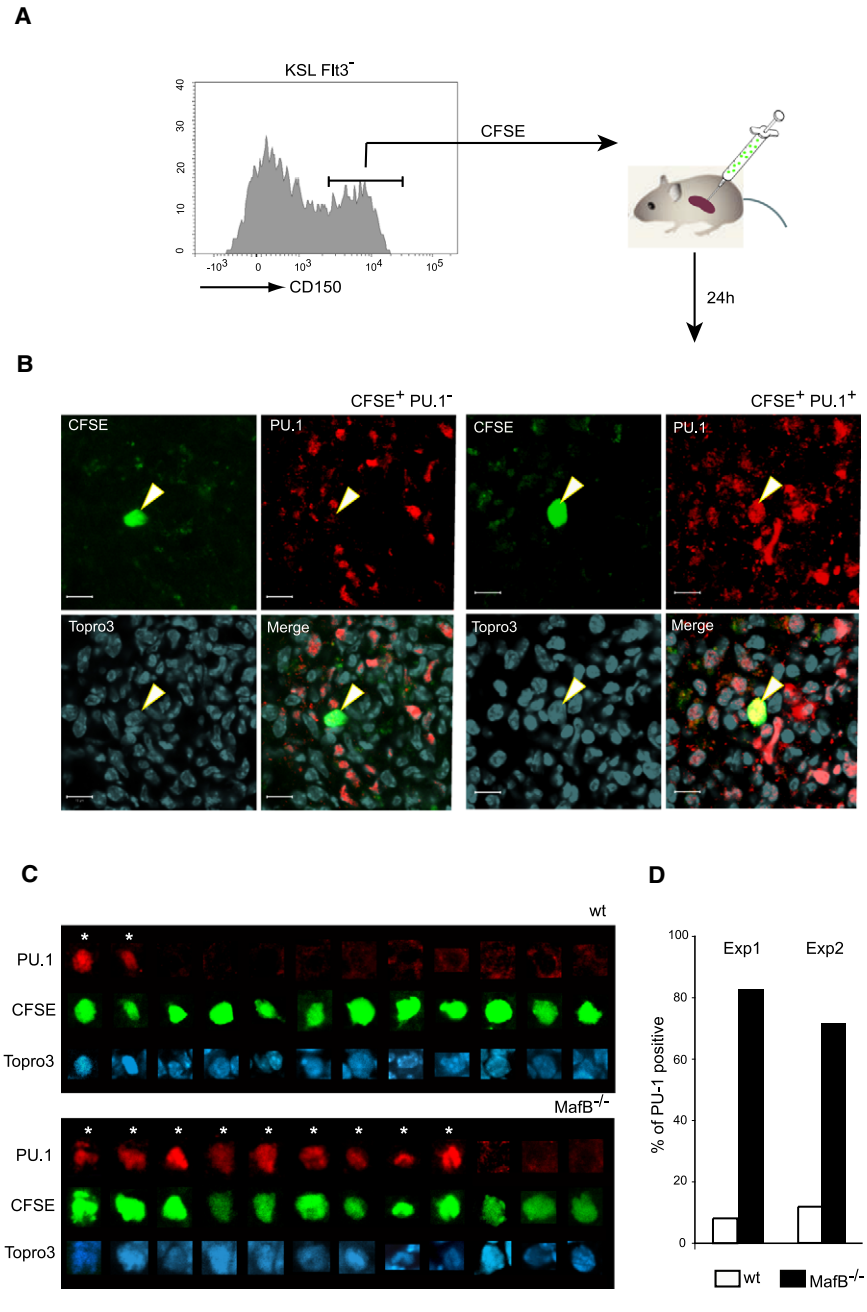

Figure 7. Increased Myeloid Commitment of *MafB*$^{-/-}$ HSCs In Vivo

(A) Experimental strategy: CSFE-labeled HSCs (CD150^{+} KSLF) were directly injected into the spleen, which was recovered after 24 hr for immunofluorescence staining.

(B) Representative examples of anti-PU.1 staining (red) on sections containing a CSFE^{+} cell (green), showing CFSE^{+} PU.1^{-} (left) and CFSE^{+} PU.1^{+} (right) cells. Nuclear topro3, gray. Scale bars represent 10 μm.

(C) Representative selection of individual PU.1^{+} and PU.1^{-} cells from spleens injected with WT or *MafB*$^{-/-}$ HSCs showing anti-PU.1 staining (red), CFSE label (green), and nuclear topro3 (blue).

(D) Quantification of two independent experiments showing the percentage of PU.1^{+} cells of WT (Exp1, n = 12; Exp2, n = 47) and *MafB*$^{-/-}$ (Exp1, n = 23; Exp2, n = 49) CFSE^{+} cells from 40 sections per spleen.

For analysis of HSCs in vivo, 3500 to 7000 FACS-sorted CD150^{+} KSLF were stained for 10 min at 37°C with 4 μM CFSE (Invitrogen) in PBS/0.5% BSA, washed 3× in PBS/0.5% BSA, and injected in 30 μl PBS into the spleen of anesthetized mice. After 24 hr, spleens were embedded in OCT (Tissue-Tek, Sakura) and frozen at −80°C. Cryostat sections (10 μm) were dried and fixed for 10 min in 4% PFA/PBS at room temperature. After washes in PBS, slides were blocked for 1 hr at room temperature in PBS/2% BSA/1% donkey serum/1% FCS/0.1% saponin, incubated for 36 hr at 4°C with anti-PU.1 polyclonal antibody (Santa Cruz) in PBS/0.05% saponin (1:50), washed, and incubated with secondary Alexa 546-donkey-anti-rabbit antibody (Molecular Probes) in PBS/0.05% saponin (1:500) and Torpo-3 (1:1000, Invitrogen). Slides were analyzed by confocal microscopy on a Zeiss LSM510 Meta. All IF samples were mounted with ProLong Gold antifade (Molecular Probes).

Proliferation Assays and Cell-Cycle Analysis

Cell cultures were incubated for 1 hr with 10 μM BrdU in appropriate medium. For in vivo analysis, BM cells were harvested 16 hr after IV injection of 5 μg rM-CSF and incubated for 1 hr at 37°C in SCM/10 μM BrdU. Using a BrdU flow kit (Becton Dickinson) and following the manufacturer's instructions, after surface marker staining and fixation, we labeled cells for 20 min at room temperature with anti-BrdU antibody, incubated with 7-AAD for 10 min at room temperature, and analyzed by FACS. For cell-cycle analysis of KSL subpopulations, BM cells were incubated for 30 min at 37°C in SCM containing 5 μM Hoechst 34580 (Invitrogen)

(1:200), washed 2× in P buffer, and incubated for 30 min with Alexa488-donkey-anti-rabbit antibody (Molecular probes) in P buffer (1:1000). Finally, cells were washed 2× in PBS, resuspended in 6 μl PBS, and dried to a glass slide for 2 min at 37°C. From randomly chosen cells in the DAPI channel, green fluorescent images were acquired under identical settings with a Zeiss Axioplan2 and SmartCapture2 software.

(D) Extracts from HEK293 cells transfected with PU.1 and different anti-PU.1 shRNA expression constructs or empty control vector (EV) were probed by western blotting for PU.1 or β-tubulin. Molecular weight is in kDa.

(E) Analysis of spleen 11 days after transplantation of Ly5.1 recipients with shPU.1/3-GFP retrovirus-infected *MafB*$^{-/-}$ (KO) Ly5.2 fetal liver cells and WT F1 competitor cells. Representative FACS profiles of KO donor and WT competitor contribution to Mac-1^{+} myeloid cells in GFP^{-} (blue) or shPU.1/3-GFP-infected GFP^{+} populations (green) and quantification of KO:WT ratios in GFP^{-} and GFP^{+} populations of Mac-1^{+} and Mac-1^{-} spleen cells (n = 3).

Error bars indicate the standard error of the mean.

before staining for cell surface markers and analysis of DNA content by FACS.

SUPPLEMENTAL DATA

Supplemental Data include Supplemental Experimental Procedures, eight figures, and one table and can be found with this article online at http://www.cell.com/supplemental/S0092-8674(09)00518-2.

ACKNOWLEDGMENTS

S.S. received fellowships from the Fondation de France (FdF) and Société Française d'Hématologie, T.F. from the European Molecular Biology Organisation and INSERM, and A.A. and L.V. from the French Ministère de l'Enseignement Supérieur et de la Recherché. We gratefully acknowledge financial support by grants from the Association pour la Recherche sur le Cancer (3857 and 3422), Association for International Cancer Research (05-0079), FdF (2004004150), and Agence Nationale de la Recherche (BLAN07-1_205752). We thank L. Rohrschneider, R.P. Bourette, G. Mouchiroud, and R. Tsien for reagents, P. Grenot, M. Barad, N. Brun, and A. Zouine for expert flow cytometry, L. Chasson from RIO/Marseille-Nice Genopole platform for histology support, F. Diaz and the Maina group for mouse handling, E. Bertosio for blood counts, and F. Rossi, T. Graf, M. Djabali, U. Nehrbass, F. Morlé, and M.H.S. group members for fruitful discussions.

Received: February 2, 2008
Revised: February 18, 2009
Accepted: April 24, 2009
Published: July 23, 2009

REFERENCES

Adams, G.B., and Scadden, D.T. (2006). The hematopoietic stem cell in its place. Nat. Immunol. *7*, 333–337.

Akashi, K., He, X., Chen, J., Iwasaki, H., Niu, C., Steenhard, B., Zhang, J., Haug, J., and Li, L. (2003). Transcriptional accessibility for genes of multiple tissues and hematopoietic lineages is hierarchically controlled during early hematopoiesis. Blood *101*, 383–389.

Arinobu, Y., Mizuno, S., Chong, Y., Shigematsu, H., Iino, T., Iwasaki, H., Graf, T., Mayfield, R., Chan, S., Kastner, P., et al. (2007). Reciprocal activation of GATA-1 and PU.1 marks initial specification of hematopoietic stem cells into myeloerythroid and myelolymphoid lineages. Cell Stem Cell *1*, 416–427.

Aziz, A., Vanhille, L., Mohideen, P., Kelly, L.M., Otto, C., Bakri, Y., Mossadegh, N., Sarrazin, S., and Sieweke, M.H. (2006). Development of macrophages with altered actin organization in the absence of MafB. Mol. Cell. Biol. *26*, 6808–6818.

Bakri, Y., Sarrazin, S., Mayer, U.P., Tillmanns, S., Nerlov, C., Boned, A., and Sieweke, M.H. (2005). Balance of MafB and PU.1 specifies alternative macrophage or dendritic cell fate. Blood *105*, 2707–2716.

Blanchi, B., Kelly, L.M., Viemari, J.C., Lafon, I., Burnet, H., Bevengut, M., Tillmanns, S., Daniel, L., Graf, T., Hilaire, G., et al. (2003). MafB deficiency causes defective respiratory rhythmogenesis and fatal central apnea at birth. Nat. Neurosci. *6*, 1091–1100.

Bourette, R.P., Grasset, M.F., and Mouchiroud, G. (2007). E2a/Pbx1 oncogene inhibits terminal differentiation but not myeloid potential of pro-T cells. Oncogene *26*, 234–247.

Bryder, D., Rossi, D.J., and Weissman, I.L. (2006). Hematopoietic stem cells: the paradigmatic tissue-specific stem cell. Am. J. Pathol. *169*, 338–346.

Carlberg, K., and Rohrschneider, L. (1994). The effect of activating mutations on dimerization, tyrosine phosphorylation and internalization of the macrophage colony stimulating factor receptor. Mol. Biol. Cell *5*, 81–95.

Chang, H.H., Hemberg, M., Barahona, M., Ingber, D.E., and Huang, S. (2008). Transcriptome-wide noise controls lineage choice in mammalian progenitor cells. Nature *453*, 544–547.

DeKoter, R.P., and Singh, H. (2000). Regulation of B lymphocyte and macrophage development by graded expression of PU.1. Science *288*, 1439–1441.

Dykstra, B., Kent, D., Bowie, M., McCaffrey, L., Hamilton, M., Lyons, K., Lee, S.-J., Brinkman, R., and Eaves, C.J. (2007). Long-term propagation of distinct hematopoietic differentiation programs in vivo. Cell Stem Cell *1*, 218–229.

Eichmann, A., Grapin-Botton, A., Kelly, L., Graf, T., Le Douarin, N.M., and Sieweke, M. (1997). The expression pattern of the mafB/kr gene in birds and mice reveals that the kreisler phenotype does not represent a null mutant. Mech. Dev. *65*, 111–122.

Enver, T., Heyworth, C.M., and Dexter, T.M. (1998). Do stem cells play dice? Blood *92*, 348–351.

Gemelli, C., Montanari, M., Tenedini, E., Zanocco Marani, T., Vignudelli, T., Siena, M., Zini, R., Salati, S., Tagliafico, E., Manfredini, R., et al. (2006). Virally mediated MafB transduction induces the monocyte commitment of human CD34+ hematopoietic stem/progenitor cells. Cell Death Differ. *13*, 1686–1696.

Hu, M., Krause, D., Greaves, M., Sharkis, S., Dexter, M., Heyworth, C., and Enver, T. (1997). Multilineage gene expression precedes commitment in the hemopoietic system. Genes Dev. *11*, 774–785.

Iwama, A., Oguro, H., Negishi, M., Kato, Y., Morita, Y., Tsukui, H., Ema, H., Kamijo, T., Katoh-Fukui, Y., Koseki, H., et al. (2004). Enhanced self-renewal of hematopoietic stem cells mediated by the polycomb gene product Bmi-1. Immunity *21*, 843–851.

Iwasaki, H., and Akashi, K. (2007). Myeloid lineage commitment from the hematopoietic stem cell. Immunity *26*, 726–740.

Jordan, C.T., and Lemischka, I.R. (1990). Clonal and systemic analysis of long-term hematopoiesis in the mouse. Genes Dev. *4*, 220–232.

Kelly, L.M., Englmeier, U., Lafon, I., Sieweke, M.H., and Graf, T. (2000). MafB is an inducer of monocytic differentiation. EMBO J. *19*, 1987–1997.

Kiel, M.J., and Morrison, S.J. (2008). Uncertainty in the niches that maintain haematopoietic stem cells. Nat. Rev. Immunol. *8*, 290–301.

Knoblich, J.A. (2008). Mechanisms of asymmetric stem cell division. Cell *132*, 583–597.

Kondo, M., Scherer, D.C., Miyamoto, T., King, A.G., Akashi, K., Sugamura, K., and Weissman, I.L. (2000). Cell-fate conversion of lymphoid-committed progenitors by instructive actions of cytokines. Nature *407*, 383–386.

Kriegler, A.B., Verschoor, S.M., Bernardo, D., and Bertoncello, I. (1994). The relationship between different high proliferative potential colony-forming cells in mouse bone marrow. Exp. Hematol. *22*, 432–440.

Lagasse, E., and Weissman, I.L. (1997). Enforced expression of Bcl-2 in monocytes rescues macrophages and partially reverses osteopetrosis in op/op mice. Cell *89*, 1021–1031.

Lo Celso, C., Fleming, H.E., Wu, J.W., Zhao, C.X., Miake-Lye, S., Fujisaki, J., Cote, D., Rowe, D.W., Lin, C.P., and Scadden, D.T. (2009). Live-animal tracking of individual haematopoietic stem/progenitor cells in their niche. Nature *457*, 92–96.

Luc, S., Buza-Vidas, N., and Jacobsen, S.E. (2008). Delineating the cellular pathways of hematopoietic lineage commitment. Semin. Immunol. *20*, 213–220.

McArthur, G.A., Rohrschneider, L.R., and Johnson, G.R. (1994). Induced expression of c-fms in normal hematopoietic cells shows evidence for both conservation and lineage restriction of signal transduction in response to macrophage colony-stimulating factor. Blood *83*, 972–981.

Metcalf, D. (1998). Lineage commitment and maturation in hematopoietic cells: the case for extrinsic regulation. Blood *92*, 345–347.

Metcalf, D. (2007). On hematopoietic stem cell fate. Immunity *26*, 669–673.

Metcalf, D. (2008). Hematopoietic cytokines. Blood *111*, 485–491.

Miyamoto, T., Iwasaki, H., Reizis, B., Ye, M., Graf, T., Weissman, I.L., and Akashi, K. (2002). Myeloid or lymphoid promiscuity as a critical step in hematopoietic lineage commitment. Dev. Cell *3*, 137–147.

Morrison, S.J., and Kimble, J. (2006). Asymmetric and symmetric stem-cell divisions in development and cancer. Nature *441*, 1068–1074.

Muller-Sieburg, C.E., Cho, R.H., Thoman, M., Adkins, B., and Sieburg, H.B. (2002). Deterministic regulation of hematopoietic stem cell self-renewal and differentiation. Blood *100*, 1302–1309.

Orford, K.W., and Scadden, D.T. (2008). Deconstructing stem cell self-renewal: genetic insights into cell-cycle regulation. Nat. Rev. Genet. *9*, 115–128.

Orkin, S.H., and Zon, L.I. (2008). Hematopoiesis: an evolving paradigm for stem cell biology. Cell *132*, 631–644.

Pawlak, G., Grasset, M.F., Arnaud, S., Blanchet, J.P., and Mouchiroud, G. (2000). Receptor for macrophage colony-stimulating factor transduces a signal decreasing erythroid potential in the multipotent hematopoietic EML cell line. Exp. Hematol. *28*, 1164–1173.

Pixley, F.J., and Stanley, E.R. (2004). CSF-1 regulation of the wandering macrophage: complexity in action. Trends Cell Biol. *14*, 628–638.

Ryan, G.R., Dai, X.-M., Dominguez, M.G., Tong, W., Chuan, F., Chisholm, O., Russell, R.G., Pollard, J.W., and Stanley, E.R. (2001). Rescue of the colony-stimulating factor 1 (CSF-1)-nullizygous mouse (Csf1op/Csf1op) phenotype with a CSF-1 transgene and identification of sites of local CSF-1 synthesis. Blood *98*, 74–84.

Schmitt, T.M., and Zuniga-Pflucker, J.C. (2002). Induction of T cell development from hematopoietic progenitor cells by delta-like-1 in vitro. Immunity *17*, 749–756.

Sieweke, M.H., and Graf, T. (1998). A transcription factor party during blood cell differentiation. Curr. Opin. Genet. Dev. *8*, 545–551.

Sieweke, M.H., Tekotte, H., Frampton, J., and Graf, T. (1996). MafB is an interaction partner and repressor of Ets-1 that inhibits erythroid differentiation. Cell *85*, 49–60.

Siminovitch, L., Till, J.E., and McCulloch, E.A. (1964). Decline in colony-forming ability of marrow cells Subjected to Serial Transplantation into Irradiated Mice. J. Cell. Physiol. *64*, 23–31.

Takano, H., Ema, H., Sudo, K., and Nakauchi, H. (2004). Asymmetric division and lineage commitment at the level of hematopoietic stem cells: inference from differentiation in daughter cell and granddaughter cell pairs. J. Exp. Med. *199*, 295–302.

Tillmanns, S., Otto, C., Jaffray, E., Duroure, C., Bakri, Y., Vanhille, L., Sarrazin, S., Hay, R.T., and Sieweke, M.H. (2007). SUMO-modification regulates MafB driven macrophage differentiation by enabling Myb dependent transcriptional repression. Mol. Cell. Biol. *27*, 5554–5564.

Wilson, A., and Trumpp, A. (2006). Bone-marrow haematopoietic-stem-cell niches. Nat. Rev. Immunol. *6*, 93–106.

Wilson, A., Laurenti, E., Oser, G., van der Wath, R.C., Blanco-Bose, W., Jaworski, M., Offner, S., Dunant, C.F., Eshkind, L., Bockamp, E., et al. (2008). Hematopoietic stem cells reversibly switch from dormancy to self-renewal during homeostasis and repair. Cell *135*, 1118–1129.

Wu, M., Kwon, H.Y., Rattis, F., Blum, J., Zhao, C., Ashkenazi, R., Jackson, T.L., Gaiano, N., Oliver, T., and Reya, T. (2007). Imaging hematopoietic precursor division in real time. Cell Stem Cell *1*, 541–554.

Xie, Y., Chen, C., and Hume, D.A. (2001). Transcriptional regulation of c-fms gene expression. Cell Biochem. Biophys. *34*, 1–16.

Zandstra, P.W., Lauffenburger, D.A., and Eaves, C.J. (2000). A ligand-receptor signaling threshold model of stem cell differentiation control: a biologically conserved mechanism applicable to hematopoiesis. Blood *96*, 1215–1222.

Zhang, C.C., and Lodish, H.F. (2008). Cytokines regulating hematopoietic stem cell function. Curr. Opin. Hematol. *15*, 307–311.

Zon, L.I. (2008). Intrinsic and extrinsic control of haematopoietic stem-cell self-renewal. Nature *453*, 306–313.